Working Paper Series, N. 3, September 2018

Department of Statistical Sciences
University of Padua
Italy

Interaction among three competitors: An extended innovation diffusion model

Claudia Furlan, Cinzia Mortarino, Mohammad Salim Zahangir
Department of Statistical Sciences
University of Padua
Italy

Abstract: In this paper, we propose a model to describe the mutual interactions among the lifecycles of three competing products acting simultaneously in a common market. To date, the literature only describes models for two competitors; therefore, the present work represents the first attempt at creating and implementing a model for three actors. The new model is applied to real data in the energy context, and its performance is compared to the performance of current models for two competitors. Regarding the datasets examined, the new model shows a relevant improvement in terms of forecasting performance, that is forecasting accuracy and prediction confidence band width.

Keywords: competition, nonlinear regression, forecasting accuracy, energy markets

UNIVERSITÀ DEGLI STUDI DI PADOVA
DIPARTIMENTO DI SCIENZE STATISTICHE

Contents

Department of Statistical Sciences
Via Cesare Battisti, 241
35121 Padova
Italy

tel: +39 049 8274168
fax: +39 049 8274170
`http://www.stat.unipd.it`

Corresponding author:
Cinzia Mortarino
tel: +39 049 827 4184
`mortarino@stat.unipd.it`
`http://www.stat.unipd.it/~mortarino`

Interaction among three competitors: An extended innovation diffusion model

Claudia Furlan, Cinzia Mortarino, Mohammad Salim Zahangir
Department of Statistical Sciences
University of Padua
Italy

Abstract: In this paper, we propose a model to describe the mutual interactions among the lifecycles of three competing products acting simultaneously in a common market. To date, the literature only describes models for two competitors; therefore, the present work represents the first attempt at creating and implementing a model for three actors. The new model is applied to real data in the energy context, and its performance is compared to the performance of current models for two competitors. Regarding the datasets examined, the new model shows a relevant improvement in terms of forecasting performance, that is forecasting accuracy and prediction confidence band width.

Keywords: competition, nonlinear regression, forecasting accuracy, energy markets

1 Introduction

Diffusion of innovations has been well researched (Peres et al., 2010), but most studies approach the topic with separate analyses for specific products or or global categories. Only in the last years (Guseo and Mortarino, 2014 and references cited therein), have some models being created to jointly describe the diffusion of two competitors simultaneously filling the same category niche. The relevance of building a *joint* model is based on the need to simultaneously estimate the peculiarities of each product and their mutual interaction that may generate competition or cooperation.

These models, either univariate or bivariate, are usually defined through a differential representation that may not admit a closed-form solution. The main advantage relies on a parsimonious description of real adoption processes based on interpretable parameters. The simplicity of the model's structure is obtained by introducing plausible assumptions regarding the behavior of the agents playing a role in the market. The relevant issue in this research topic is to build an adequately large set of models to describe the different characteristics of the diffusion process. Confirmation or rejection of the assumptions underlying each model is then attained by fitting available observed data and comparing the models' performances.

Diffusion models have been systematically applied to the energy market in the last years. It is well established in the literature that energy consumption may be represented in terms of a market, similar to commercial products (Marchetti and Nakicenovic, 1979). The main reason is that exploitation of energy sources coevolves with the development of technological innovations the diffusion of which is essential for the growth of the source itself. Univariate applications to the energy market have been undertaken in Guseo and Dalla Valle (2005), Guseo et al. (2007), Guseo (2011) (for crude oil), Guseo et al. (2015), Darda et al. (2015) (for natural gas), Dalla Valle and Furlan (2011) and Guidolin and Mortarino (2010) (for wind and PV, respectively) and Guidolin and Guseo (2012), Dalla Valle and Furlan (2014), Furlan et al. (2016) (for nuclear power).

Because countries have energy needs that can be fulfilled through alternative sources, a competition framework can describe the dynamic relative importance of each source in a realistic way. Some research involves a joint model for two series. Guidolin and Guseo (2016) focused on analysing the recent impact of renewables, examining the competition between nuclear sources and renewables in Germany but did not include information about coal, gas, and oil (CGO). Furlan and Mortarino (2018) chose a different approach; they analysed four regions and added data for nuclear sources to CGO data, to contrast fossil with non-fossil sources. The cited works are examples of applications of a bivariate competition.However, there are no published models that are feasible for more than two competitors. In other words, the extension from two to more than two actors is only theoretically included in the current literature, but high parameter dimension and complex structure of the interactions among competitors prevent this extension from being a real tool. Therefore, to obtain a bivariate structure in applications, practitioners are forced to aggregate data pertaining to more similar products or to describe the market using only the two leading actors. This, of course, leads to hiding the specific peculiarities of some of the actors, thus wasting rich information.

The aim of this paper is to contribute to the topic of modelling the diffusion of innovations to describe a market where three actors compete for the same customers, illustrating how rich the description of their mutual interactions could be to accurately represent the market's features.

Analysing real data in the energy context, we will show how a three–competitor model (3CM) can be fitted. The analysis concerns the consumption of CGO, renewables, and nuclear sources. We will also fit a reduced model for two competitors (2CM) (Guseo and Mortarino, 2014) to the same datasets whereby the data for two competitors are aggregated (that is, nuclear data are added to CGO data). The aim of the comparison is to show that using the richer dataset through the 3CM allows us to obtain better performances in terms of forecasting accuracy and/or of reducing prediction confidence band width.

Section 2 describes the 3CM together with inferential aspects and details of the procedure used here to compare the 3CM with the 2CM. The model is applied to two different countries in Section 3. Finally, concluding remarks are proposed in Section 4.

2 Model

2.1 Model definition

As mentioned above, diffusion models describe the evolution of lifecycles as growth curves defined through differential equations or systems.

Let $z_i(t)$, $i = 1, 2, 3$, be the cumulative sales up to time t of the i-th competitor, and let $z(t) = \sum_i z_i(t)$ be the category cumulative sales of all the competitors in the market. Let $z'_i(t) = dz_i(t)/dt$ be the instantaneous sales of the i-th product. Because the products represent a homogeneous category competing for the same customers, we assume a common market potential, m, and correspondingly a common residual market, $m - z(t)$.

Guseo and Mortarino (2014)'s model describes the interaction between a subset of two competitors:

$$\begin{aligned} z'_1(t) &= m\left[p_1 + (q_1 + \delta)\frac{z_1(t)}{m} + q_1\frac{z_2(t)}{m}\right] R(t)x_1(t) \\ z'_2(t) &= m\left[p_2 + (q_2 - \delta)\frac{z_1(t)}{m} + q_2\frac{z_2(t)}{m}\right] R(t)x_2(t) \\ z(t) &= z_1(t) + z_2(t), \end{aligned} \tag{1}$$

where $R(t) = 1 - z(t)/m$ represents the relative residual market for the whole category. Both products may benefit from an innovation driver (parameters p_1 and p_2) and a flexible word-of-mouth (WOM) structure (parameters q_1, q_2 and δ), differentiating an internal driver (within-brand WOM) from an external one (cross-brand WOM).

These features of the 2CM are included in its extension to three competitors. Because it is not very common to observe three products being launched simultaneously, we will focus on situations where two products exist in the market from the beginning ($t = 0$) while the third product enters the market later at time $t = c_2$, with $c_2 > 0$ (other cases can be easily dealt with). The 3CM proposed here can be expressed with the following system of differential equations:

$$\begin{aligned} z'_1(t) =& m\Bigg\{\left[p_{1\alpha} + (q_{1\alpha} + \delta_\alpha)\frac{z_1(t)}{m} + q_{1\alpha}\frac{z_2(t)}{m}\right](1 - I_{t>c_2}) + \\ &+ \left[p_{1\beta} + (q_{1\beta} + \delta_\beta)\frac{z_1(t)}{m} + q_{1\beta}\frac{z_2(t)}{m} + q_{1\beta}\frac{z_3(t)}{m}\right] I_{t>c_2}\Bigg\} R(t)x_1(t) \\ z'_2(t) =& m\Bigg\{\left[p_{2\alpha} + (q_{2\alpha} - \delta_\alpha)\frac{z_1(t)}{m} + q_{2\alpha}\frac{z_2(t)}{m}\right](1 - I_{t>c_2}) + \\ &+ \left[p_{2\beta} + q_{2\beta}\frac{z_1(t)}{m} + (q_{2\beta} + \delta_\beta)\frac{z_2(t)}{m} + q_{2\beta}\frac{z_3(t)}{m}\right] I_{t>c_2}\Bigg\} R(t)x_2(t) \\ z'_3(t) =& m\Bigg\{\left[p_3 + (q_3 - \delta_\beta)\frac{z_1(t)}{m} + (q_3 - \delta_\beta)\frac{z_2(t)}{m} + q_3\frac{z_3(t)}{m}\right] I_{t>c_2}\Bigg\} R(t)x_3(t) \\ m =& m_\alpha(1 - I_{t>c_2}) + m_\beta I_{t>c_2} \\ z(t) =& z_1(t) + z_2(t) + z_3(t) I_{t>c_2}. \end{aligned} \tag{2}$$

System (2) describes a competition among three products in two phases. During the first phase, until $t \le c_2$, it is assumed that the first two products are characterized separately by three parameters each (denoted with subscript α). The parameters of the first product are $(p_{1\alpha}, q_{1\alpha}, \delta_\alpha)$, and the parameters of the second product are $(p_{2\alpha}, q_{2\alpha}, \delta_\alpha)$. At time $t = c_2$ when the competition extends from two to three products, we allow the first two products to be characterized by new parameters (denoted with subscript β): $(p_{1\beta}, q_{1\beta}, \delta_\beta)$ for the first competitor, and $(p_{2\beta}, q_{2\beta}, \delta_\beta)$ for the second. This is an important feature, as it is very common that a new competitor's launch affects the diffusion dynamics of existing products. The third competitor is characterized by parameters (p_3, q_3, δ_β).

Parameters δ_j, $j \in \{\alpha, \beta\}$, serve the purpose of differentiating between within–brand WOM (the effect on the future adopters of a product due to its previous adoptions) and cross–brand WOM (the effect on the future adopters of a product due to the past adoptions of its competitors). Restricted models where δ_α and/or δ_β equal zero may be applied whenever data support this constraint. The common market potential, m, is equal to m_α in the first phase and is allowed to change to m_β in the second phase.

The model may also describe specific exogenous changes in the diffusion speed of each competitor using the intervention functions $x_i(t)$, $i = 1, 2, 3$, (Bass et al., 1994). These functions are flexible structures (Guseo and Dalla Valle, 2005) the parameters of which are estimated simultaneously with the diffusion parameters. For example, a sudden change, such as an exponential shock, could be modelled through

$$x_i(t) = 1 + c_i e^{b_i(t-a_i)} I_{[t \geq a_i]}, \tag{3}$$

where a_i denotes the starting time of the shock, b_i indicates how rapidly the shock decays towards 0, and c_i denotes the intensity of the shock (either positive or negative). A more regular variation within a defined time lapse could be described by a rectangular shock:

$$x_i(t) = 1 + c_i I_{[a_i \leq t \leq b_i]}, \tag{4}$$

where now a_i and b_i define the time interval when the shock affects diffusion, and c_i indicates, as before, the intensity of the shock.

2.2 Inferential aspects

To estimate all the parameters involved in diffusion models, we use the following nonlinear regression model where the observed instantaneous sales for each the three products, $s_i(t)$, are used as dependent variables:

$$s_i(t) = z_i'(t) + \varepsilon_i(t), \qquad i = 1, 2, 3, \tag{5}$$

where $z_i'(t) = z_i'(t; \vartheta)$ can be defined by the model given in Eq. (2) or equations corresponding to any other diffusion model, and $\varepsilon_i(t)$ indicates the error term. The set of parameters of the diffusion model, ϑ, can be estimated through a non-linear least square (NLS) algorithm without allowing detailed assumptions, from the beginning, about the structure of $\varepsilon_i(t)$. For further details about inference for nonlinear models, see Seber and Wild (2003).

In addition to estimating parameters, forecasting is crucial for the diffusion process. In order to predict the future values, we follow the iterative Euler method for the numerical solution of differential equations (see, e.g., Atkinson, 1962). This step is necessary because of the absence of a closed-form solution that would provide a function to be evaluated for t values outside the observation range.

To compute confidence bands for the predicted values, assumptions about the distribution of $\varepsilon_i(t)$ are required. Following Boswijk and Franses (2005), we assume a specific pattern of heteroscedasticity:

$$\varepsilon_i(t) = z_i'(t;\vartheta)u_i(t), \quad i = 1,2,3.$$

Therefore, Eq. (5) can be rewritten as

$$s_i(t) = z_i'(t;\vartheta) + z_i'(t;\vartheta)u_i(t), \quad i = 1,2,3, \tag{6}$$

where $u_i(t)$ is supposed to be normally distributed with zero mean and constant variance, ${}_u\sigma_i^2$, $i = 1,2,3$. Equation (6) provides low variability around the mean trajectory both at the beginning and at the end of the diffusion cycle, with higher variability when the diffusion peaks. This results in a more realistic description of the diffusion process.

After parameter estimation, the estimates of $u_i(t)$ can be calculated as:

$$\hat{u}_i(t) = \left[s_i(t) - z_i'(t;\hat{\vartheta})\right] / z_i'(t;\hat{\vartheta}), \quad i = 1,2,3. \tag{7}$$

We call $\hat{u}_i(t)$ 'scaled residuals'. 95% confidence bands for the predictions $\hat{z}_i(t) = z_i(t;\hat{\vartheta})$ can be computed as:

$$\hat{z}_i(t) \pm 2\ {}_u\hat{\sigma}_i\ \hat{z}_i'(t), \quad t = T+1, T+2, ..., \tag{8}$$

where ${}_u\hat{\sigma}_i^2$, $i = 1,2,3$, represent the variance estimates obtained from the scaled residuals, and T is the number of observations used to estimate the parameters (for details, see Guseo and Mortarino, 2015).

2.3 Model comparison

The relevant aspect in this research is studying to what extent a 3CM could improve the analysis of a dataset compared to a 2CM. Let us assume that the 2CM is applied to the data of Competitor 1 and to the sum of the data of Competitors 2 and 3. Because the two models being compared (2CM and 3CM) would use different data, it is not appropriate to make a direct comparison of global goodness-of-fit measures. We therefore decided to evaluate the improvement of the 3CM with respect to the 2CM, focusing on Competitor 1, which is the common element. The idea is to show that a better description of Competitor 1's rivals—obtained by separately modelling the data of Competitor 2 and Competitor 3—would result in an improved forecasting performance for Competitor 1. The forecasting performance is evaluated both by confidence band width and by forecasting accuracy measures.

Given the confidence bands definition of Eq. (8), their width is equal to:

$$4\ {}_u\hat{\sigma}_i\ \hat{z}_i'(t), \quad t = T+1, T+2, ... \tag{9}$$

This highlights that width is affected both by residuals' variability, ${}_u\hat{\sigma}_i$, and by the fitted trajectory, $\hat{z}_i'(t)$. Both may depend upon model choice, but while low residuals' variability always represents an improvement, the role of $\hat{z}_i'(t)$ may be controversial, as will be highlighted in the applications in Section 3.

Forecasting accuracy is assessed by a 'rolling-origin evaluation' process (Tashman, 2000) using a broad set of accuracy measures. Here, we use RMSE, MAPE, sMAPE, MASE (Hyndman and Koehler, 2006) and the more recent UMBRAE (Chen et al., 2017). In particular, MASE (Hyndman and Koehler, 2006) can be defined as:

$$\text{MASE} = \frac{1}{n}\sum_{t=1}^{n}\left(\frac{e_t}{\frac{1}{n-1}\sum_{i=2}^{n}|z_i - z_{i-1}|}\right), \tag{10}$$

where z_t is the observed value at time t, f_t is the corresponding forecast, and $e_t = z_t - f_t$ is the forecasting error at time t. Notice that MASE will not be infinite unless all historical data are equal. When MASE<1, errors from the proposed method are, on average, smaller than errors from the one-step random walk. The more recent proposal, UMBRAE (Chen et al., 2017), is defined as follows:

$$\text{UMBRAE} = \frac{\text{MBRAE}}{1 - \text{MBRAE}}, \tag{11}$$

where MBRAE is the average of the bounded RAE:

$$\text{BRAE} = \frac{|e_t|}{|e_t^*| + |e_t|}, \tag{12}$$

with e_t^* denoting the forecast error with the one-step random walk. When UMBRAE is equal to 1, the proposed method performs roughly the same as the naïve method. When UMBRAE $<$ ($>$)1, the proposed model performs roughly (1- UMBRAE)×100% better ((UMBRAE-1)×100% worse) than the naïve method.

3 Application and results

For the applications, we considered the yearly energy consumption (provided by British Petroleum, in Mtoe) of CGO, nuclear sources and renewables for Switzerland and Sweden, for the period 1965–2015 (British Petroleum, 2016).

The comparison concerns a model in which we separately analyse CGO, the Renewables and Nuclear data and a model to which CGO and Nuclear data are added to provide a single time series. To make a more interesting comparison, we chose countries for which nuclear energy sources are nonneglegible. Nuclear energy began being exploited in both countries a few years after the start of observation.

The main difference between the two countries is that nuclear energy has a different market share in the energy mix. For Switzerland, nuclear energy reached approximately 19% of the total consumption (28% of fossil consumption, CGON). Moreover, as shown in Figure 1, in the last two decades the relative importance of the three sources has been quite stable. Conversely, for Sweden, nuclear energy reached approximately 24% of the total consumption (43% of fossil consumption,

Table 1: Switzerland. Estimation results for the 2CM. Subscript 1 denotes CGON, while subscript 2 denotes renewables.

Parameter	Estimate	Standard error	95% Confidence interval
m	$2.2232*10^3$	$5.9118*10^1$	$(2.1057*10^3, 2.3406*10^3)$
p_1	$4.3527*10^{-3}$	$1.6297*10^{-4}$	$(4.0290*10^{-3}, 4.6765*10^{-3})$
q_1	$9.5585*10^{-2}$	$2.2560*10^{-2}$	$(5.0765*10^{-2}, 1.4040*10^{-1})$
δ	$-9.6204*10^{-2}$	$3.2372*10^{-2}$	$(-1.6052*10^{-1}, -3.1892*10^{-2})$
c_1	$2.0395*10^{-1}$	$4.9370*10^{-2}$	$(1.0587*10^{-1}, 3.0203*10^{-1})$
b_1	$-2.6374*10^{-1}$	$9.8537*10^{-2}$	$(-4.5950*10^{-1}, -6.7979*10^{-2})$
a_1	6.7213	$2.6556*10^{-3}$	(6.7160, 6.7266)
p_2	$2.8995*10^{-3}$	$1.3021*10^{-4}$	$(2.6408*10^{-3}, 3.1582*10^{-3})$
q_2	$-5.9186*10^{-2}$	$2.2940*10^{-2}$	$(-1.0476*10^{-1}, -1.3611*10^{-2})$
c_2	$1.4114*10^{-1}$	$8.4596*10^{-2}$	$(-2.6921*10^{-2}, 3.0921*10^{-1})$
b_2	$1.3846*10^{-1}$	$1.9591*10^{-1}$	$(-2.5074*10^{-1}, 5.2767*10^{-1})$
a_2	47.1195	$1.6533*10^{-3}$	(47.1162, 47.1228)
$R^2 = 0.988735$			

CGON). In the last 10 years, we observe dynamic market shares, with renewables gaining the major share (Figure 6).

For these applications, we decided to use a forecasting horizon of five years, which is a reasonable time period for the energy market. For the same reason, forecasting accuracy will be evaluated from 1 to 5-year-ahead.

3.1 Switzerland

The data are plotted in Figure 1. Nuclear consumption began slowly in 1969 and attained a long-term level around 1984. We observe that its evolution is very different from the profile observed for other fossil sources. If we had to rely only on 2CM, we would be forced to reduce to two competitors, as in Furlan and Mortarino (2018), where nuclear data have been added to CGO consumption data, to contrast fossil with non-fossil sources. We proceeded in the same way for our data, obtaining the two series plotted in Figure 2. The fitting of the data aggregated as explained to model (1) gives the results shown in Table 1, while Figure 3 highlights the fitted trajectories, predictions for five years after the observation period and the corresponding confidence bands, evaluated according to Eq. (8). In Table 1, subscript 1 denotes CGON, while subscript 2 denotes renewables. Two exponential shocks are used to improve the fitting: a positive one ($\hat{c}_1 > 0$) for CGON in 1965+$\hat{a}_1 \simeq 1972$, and a positive one ($\hat{c}_2 > 0$) for renewables starting in 1965+$\hat{a}_2 \simeq 2012$.

Let us examine now the complete dataset with the three separate time series in Figure 1. Because period α (when only CGO and renewables compete) is very short, we chose to fit a simpler version of model (2) with $\delta_\alpha = 0$. Table 2 shows the results. Here, subscript 1 denotes CGO, subscript 2 denotes renewables, and

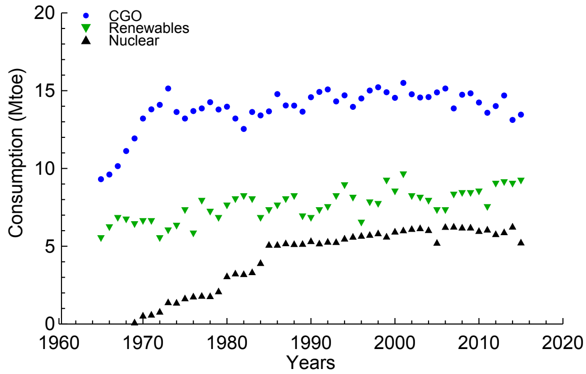

Figure 1: Switzerland. Data pertaining to the three energy sources: CGO (Coal, Gas and Oil), renewables, and nuclear.

subscript 3 denotes nuclear energy. The model includes a positive shock for CGO in $1965+\hat{a}_1 \simeq 1974$, a positive one for renewables starting in $1965+\hat{a}_2 \simeq 2013$, and a positive one for nuclear in $1965+\hat{a}_3 \simeq 1985$.

Notice that the choice among alternative nested models cannot be made by looking at marginal confidence intervals for single parameters, as, due to the curvature of the parameter space, each confidence interval represents only a specific section of the space and could be very misleading. The choice of the best model is therefore made by evaluating tests to compare nested models based on the global fitting (see Guseo and Mortarino, 2015 for details). The significance of exogenous shocks is tested with the same approach. In this case, the p-value for the test assessing the significance of the three shocks equals 0.0064. Notice that the p-value of the test to assess whether a model with δ_β=0 would provide an adequate fit is equal to 0.0147. Figure 4 shows fitted values, predictions and confidence bands for the 3CM.

Notice that estimated values for the WOM parameters $(q_{1\beta}, q_{2\beta}, q_{3\beta}, \delta_\beta)$ allow for an interesting interpretation of the interaction among the three energy sources. Substitution of the estimates into model (2) leads to the following equations:

$$
\begin{aligned}
z_1'(t)I_{t>c_2} &\propto \left[0.0049 - 0.0004\frac{z_1(t)}{m} + 0.0250\frac{z_2(t)}{m} + 0.0250\frac{z_3(t)}{m}\right] \\
z_2'(t)I_{t>c_2} &\propto \left[0.0024 + 0.0147\frac{z_1(t)}{m} - 0.0108\frac{z_2(t)}{m} + 0.0147\frac{z_3(t)}{m}\right] \\
z_3'(t)I_{t>c_2} &\propto \left[-0.0003 + 0.0137\frac{z_1(t)}{m} + 0.0137\frac{z_2(t)}{m} - 0.0117\frac{z_3(t)}{m}\right].
\end{aligned}
$$

These equations describe a very competitive context where internal WOM is negative and the consumption of each source is fostered by external pressure (e.g., the diffusion of renewables is stimulated by CGO and nuclear consumption).

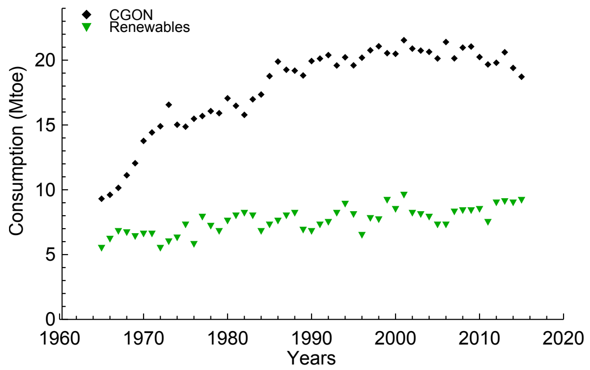

Figure 2: Switzerland. Data obtained from the aggregation of fossil fuels: CGON (Coal, Gas, Oil and Nuclear) and renewables.

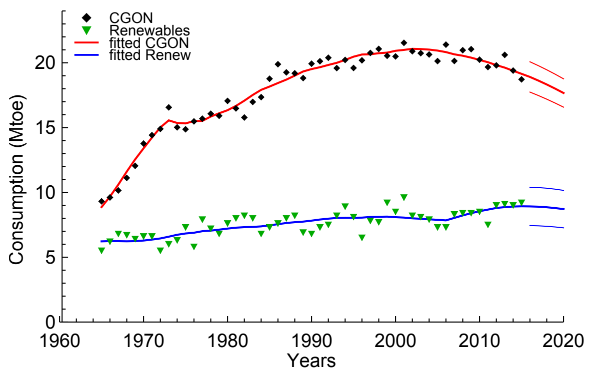

Figure 3: Switzerland. Data and fitted values for the 2CM, system (1).

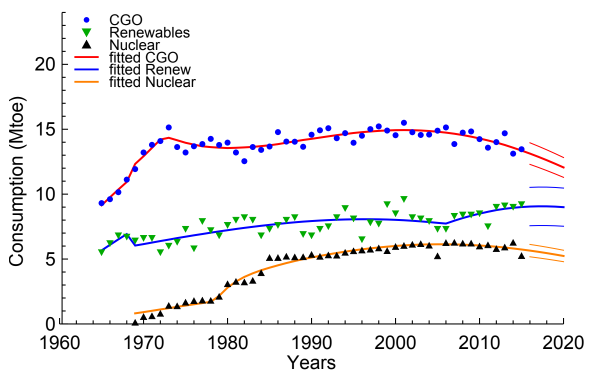

Figure 4: Switzerland. Data and fitted values for the 3CM, system (2).

Table 2: Switzerland. Estimation results for the 3CM. Subscript 1 denotes CGO, subscript 2 denotes renewables and subscript 3 denotes nuclear.

Parameter	Estimate	Standard error	95% confidence interval
m_α	5.6640∗10^{2}	2.5184∗10^{-8}	(5.6634∗10^{2}, 5.6640∗10^{2})
$p_{1\alpha}$	1.6178∗10^{-2}	7.4599∗10^{-4}	(1.4701∗10^{-2}, 1.7654∗10^{-2})
$q_{1\alpha}$	3.8451∗10^{-2}	1.4468∗10^{-2}	(9.8220∗10^{-3}, 6.7080∗10^{-2})
m_β	2.6052∗10^{3}	1.3844∗10^{2}	(2.3312∗10^{3}, 2.8791∗10^{3})
$p_{1\beta}$	4.8964∗10^{-3}	2.4657∗10^{-4}	(4.4085∗10^{-3}, 5.3843∗10^{-3})
$q_{1\beta}$	2.5030∗10^{-2}	5.8230∗10^{-3}	(1.3507∗10^{-2}, 3.6552∗10^{-2})
δ_β	-2.5424∗10^{-2}	1.0066∗10^{-2}	(-4.5343∗10^{-2}, -5.5050∗10^{-3})
c_1	2.6752∗10^{-1}	1.5234∗10^{-1}	(-3.3927∗10^{-2}, 5.6896∗10^{-1})
b_1	-1.8912	1.8674	(-5.5863, 1.8040)
a_1	8.6553	7.7069∗10^{-2}	(8.5028, 8.8078)
$p_{2\alpha}$	1.0018∗10^{-2}	7.4599∗10^{-4}	(8.5417∗10^{-3}, 1.1494∗10^{-2})
$q_{2\alpha}$	2.6544∗10^{-2}	1.4468∗10^{-2}	(-2.0851∗10^{-3}, 5.5173∗10^{-2})
$p_{2\beta}$	2.3531∗10^{-3}	1.3310∗10^{-4}	(2.0898∗10^{-3}, 2.6165∗10^{-3})
$q_{2\beta}$	1.4661∗10^{-2}	3.1345∗10^{-3}	(8.4584∗10^{-3}, 2.0864∗10^{-2})
c_2	1.2913∗10^{-1}	6.3375∗10^{-2}	(3.7244∗10^{-3}, 2.5454∗10^{-1})
b_2	8.7119∗10^{-2}	1.9123∗10^{-1}	(-2.9129∗10^{-1}, 4.6553∗10^{-1})
a_2	47.5553	7.1297∗10^{-4}	(47.5539, 47.5567)
p_3	-2.6718∗10^{-4}	1.5258∗10^{-4}	(-5.6911∗10^{-4}, 3.4743∗10^{-5})
q_3	-1.1736∗10^{-2}	8.2234∗10^{-3}	(-2.8009∗10^{-2}, 4.5365∗10^{-3})
c_3	4.1973∗10^{-1}	1.2489∗10^{-1}	(1.7260∗10^{-1}, 6.6686∗10^{-1})
b_3	-1.0201∗10^{-1}	5.2892∗10^{-2}	(-2.0668∗10^{-1}, 2.6512∗10^{-3})
a_3	20.0000	5.3474∗10^{-3}	(19.9894, 20.0106)
$R^2 = 0.987098$			

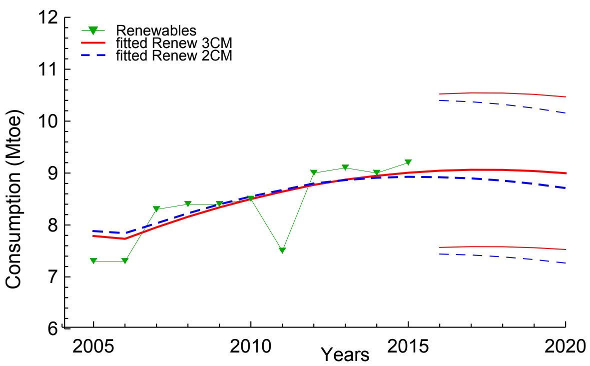

Figure 5: Switzerland. Predictions and confidence bands for renewables for 3CM and 2CM.

Table 3: Switzerland. Comparison between 2CM and 3CM: confidence band width, estimated standard deviation and p-value for the Kolmogorov–Smirnov test.

		2CM	3CM
$_u\hat{\sigma}_2$		0.0827	0.0801
p-value		0.9310	0.9586
confidence band width	step 1	3.0497	2.9349
	step 2	3.0799	2.9478
	step 3	3.1160	2.9618
	step 4	3.1585	2.9770
	step 5	3.2081	2.9936

Table 4: Switzerland. Comparison between 2CM and 3CM: forecasting accuracy measures.

Renewables	2CM					3CM				
	step 1	step 2	step 3	step 4	step 5	step 1	step 2	step 3	step 4	step 5
RMSE	1.604	1.976	2.260	2.763	2.368	1.287	1.653	1.891	2.225	1.959
MAPE	0.059	0.075	0.100	0.149	0.150	0.043	0.064	0.085	0.121	0.124
sMAPE	0.061	0.078	0.106	0.162	0.162	0.044	0.066	0.088	0.129	0.132
MASE	0.831	1.066	1.446	2.213	2.220	0.590	0.905	1.210	1.796	1.836
UMBRAE	2.095	2.042	1.146	1.713	2.044	0.994	1.759	0.779	1.404	1.689
% Better	29%	33%	40%	0%	0%	71%	33%	60%	25%	0%

3.1.1 Comparison between 2CM and 3CM

The comparison between 2CM and 3CM can be achieved, as a first step, by examining $_u\hat{\sigma}_2$ values, the estimated standard deviation for scaled residuals, for the renewables as indicators of global fit.

Moreover, to show the forecasting performance, Figure 5 highlights the final part of the series and the fitted values with 5-step-ahead forecasts obtained with 3CM and 2CM for renewables, the element common to the two models. To confirm the hypothesis that scaled residuals follow a Gaussian distribution, we use the Kolmogorov–Smirnov test for normality. Table 3 shows confidence band width for the two models, together with $_u\hat{\sigma}_2$ and the p-values for the Kolmogorov–Smirnov normality test. For both models, the hypothesis of Gaussian residuals is confirmed by the data. The 3CM shows a smaller value for $_u\hat{\sigma}_2$ and gives a reduction in terms of confidence band width for forecasts from 1-step-ahead to 5-step-ahead.

Forecasting accuracy analysis results are given in Table 4. The results are uncontroversial because all the evaluated measures have smaller values for the 3CM if compared with the 2CM at each of the 5 steps. This highlights that the richer model exploiting a better description of CGO and nuclear results also in a better forecasting performance for renewables.

Table 5: Sweden. Estimation results for the 2CM. Subscript 1 denotes CGON, subscript 2 denotes renewables.

Parameter	Estimate	Standard error	95% Confidence interval
m	$3.4990*10^3$	$4.1887*10^2$	$(2.6668*10^3, 4.3311*10^3)$
p_1	$6.3295*10^{-3}$	$8.5302*10^{-4}$	$(4.6348*10^{-3}, 8.0242*10^{-3})$
q_1	$1.3153*10^{-1}$	$6.6846*10^{-2}$	$(-1.2689*10^{-3}, 2.6434*10^{-1})$
δ	$-1.6301*10^{-1}$	$9.0863*10^{-2}$	$(-3.4352*10^{-1}, 1.751*10^{-2})$
c_1	$2.112*10^{-1}$	$6.5880*10^{-2}$	$(8.0320*10^{-2}, 3.4208*10^{-1})$
b_1	$1.5685*10^{-2}$	$2.5868*10^{-2}$	$(-3.5706*10^{-2}, 6.7077*10^{-2})$
a_1	3.1165	$2.1825*10^{-4}$	(3.1161, 3.1169)
p_2	$2.7314*10^{-3}$	$3.2021*10^{-4}$	$(2.0953*10^{-3}, 3.3676*10^{-3})$
q_2	$-1.0260*10^{-1}$	$6.4305*10^{-2}$	$(-2.3035*10^{-1}, 2.5158*10^{-2})$
c_2	$5.2541*10^{-2}$	$3.1005*10^{-2}$	$(-9.0567*10^{-3}, 1.1414*10^{-1})$
b_2	$1.7576*10^{-1}$	$2.6149*10^{-2}$	$(1.2381*10^{-1}, 2.2771*10^{-1})$
a_2	33.1467	$2.8633*10^{-4}$	(33.1461, 33.1473)
$R^2 = 0.975056$			

3.2 Sweden

The data are plotted in Figure 6. Nuclear sources began to be used in Sweden in 1972. For this country, nuclear and renewable sources represent a relevant contribution in the energy mix, and in the last years these sources overtook CGO in terms of consumptions. The paths of the three competitors are very different. If we add data for nuclear to CGO data, we obtain the two series plotted in Figure 7. The fitting of the data aggregated as explained to model (1) gives the results shown in Table 5, while Figure 8 highlights the fitted trajectories, predictions for five years after the observation period and the corresponding confidence bands, evaluated according to Eq. (8). Two shocks are included in the model: a positive one affecting CGON in $1965+\hat{a}_1 \simeq 1968$ and a positive one in $1965+\hat{a}_2 \simeq 1998$ affecting renewables.

Table 6 shows the results for model (2) for the complete dataset with three separate competitors (the constraint $\delta_\alpha = \delta_\beta = 0$ proved to be restrictive for these data, p-value=0.0123). Separating the sources also allowed recognizing specific shocks for the three series: a negative shock for CGO in $1965+\hat{a}_1 \simeq 1982$, a positive one for renewables starting in $1965+\hat{a}_2 \simeq 1999$, and a positive one for nuclear in $1965+\hat{a}_3 \simeq 1986$ (when the Chernobyl disaster occurred). In this case, the p-value for the test assessing the significance of the three shocks equals 5.5×10^{-5}. Figure 9 shows fitted values, predictions and confidence bands.

The interpretation of parameters highlights an interaction among the three energy sources similar to the one described for Switzerland. Substitution of the esti-

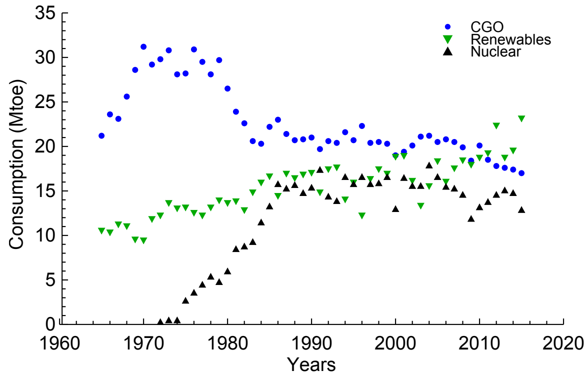

Figure 6: Sweden. Data pertaining to the three energy sources: CGO (Coal, Gas and Oil), renewables, and nuclear.

mates into model (2) leads to the following equations:

$$\begin{aligned}
z_1'(t)I_{t>c_2} &\propto \left[0.0087 - 0.0239\frac{z_1(t)}{m} + 0.0404\frac{z_2(t)}{m} + 0.0404\frac{z_3(t)}{m}\right] \\
z_2'(t)I_{t>c_2} &\propto \left[0.0025 + 0.0297\frac{z_1(t)}{m} - 0.0346\frac{z_2(t)}{m} + 0.0297\frac{z_3(t)}{m}\right] \\
z_3'(t)I_{t>c_2} &\propto \left[-0.0022 + 0.0307\frac{z_1(t)}{m} + 0.0307\frac{z_2(t)}{m} - 0.0336\frac{z_3(t)}{m}\right].
\end{aligned}$$

As for Switzerland, internal WOM is negative and the consumption of each source is fostered by external pressure. All these effects are even stronger for Sweden, as the magnitude of the coefficients is larger than we observed for Switzerland. We could say that for both countries, larger values for the consumption of any source stimulate the need to promote alternative sources. This is unsurprising due to the increased perceived uncertainty regarding the provision of energy in recent years, especially for countries that are not self-sufficient.

3.2.1 Comparison between 2CM and 3CM

Figure 10 highlights the final part of the series and the fitted values with 5-step-ahead forecasts obtained with 3CM and 2CM for renewables, the element common to the two models. Table 7 shows confidence band width for the two models, together with ${}_u\hat{\sigma}_2$, the estimated standard deviation for scaled residuals for renewables, and the p-values for the Kolmogorov–Smirnov normality test. For both models, the hypothesis of Gaussian residuals is confirmed by the data. As we anticipated in Subsection 2.3, the band width results require a specific comment. The 3CM apparently results in a reduction in terms of confidence band width only for 1- and 2-step-ahead forecasts. Both ${}_u\hat{\sigma}_2$ values and Figure 10 highlight, however, that the slight increase for 3-step-ahead and further is due to the steep increase in the predicted trajectory for the 3CM in contrast to a mild increase in the 2CM fitted trajectory. Conversely, ${}_u\hat{\sigma}_2$ has a lower value for the 3CM, showing greater precision.

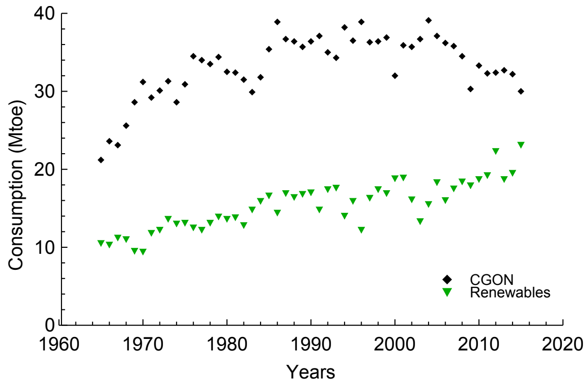

Figure 7: Sweden. Data obtained from the aggregation of fossil fuels: CGON (Coal, Gas, Oil and Nuclear) and renewables.

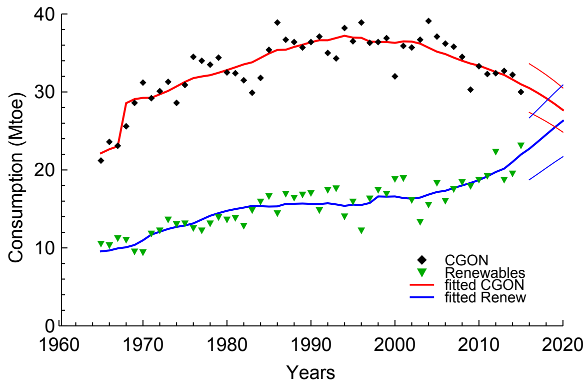

Figure 8: Sweden. Data and fitted values for the 2CM, system (1).

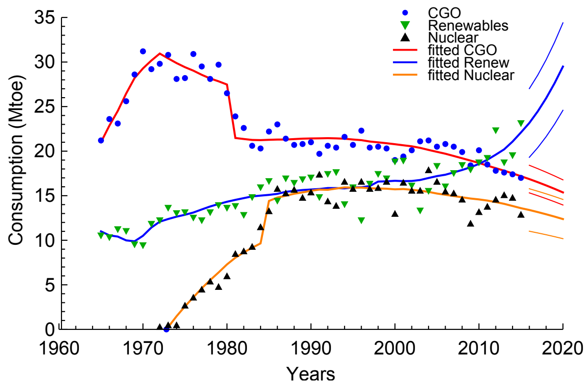

Figure 9: Sweden. Data and fitted values for the 3CM, system (2).

Table 6: Sweden. Estimation results for the 3CM. Subscript 1 denotes CGO, subscript 2 denotes renewables and subscript 3 denotes nuclear.

Parameter	Estimate	Standard error	95% Confidence interval
m_α	$1.4598*10^{3}$	$7.0211*10^{-9}$	$(1.4598*10^{3}, 1.4598*10^{3})$
$p_{1\alpha}$	$1.4383*10^{-2}$	$6.2848*10^{-4}$	$(1.3139*10^{-2}, 1.5627*10^{-2})$
$q_{1\alpha}$	$3.0682*10^{-1}$	$1.7885*10^{-1}$	$(-4.7205*10^{-2}, 6.6084*10^{-1})$
δ_α	$-3.7089*10^{-1}$	$2.5191*10^{-1}$	$(-8.6952*10^{-1}, 1.2775*10^{-1})$
m_β	$3.9419*10^{3}$	$5.8051*10^{2}$	$(2.7928*10^{3}, 5.0910*10^{3})$
$p_{1\beta}$	$8.7467*10^{-3}$	$1.1363*10^{-3}$	$(6.4976*10^{-3}, 1.0996*10^{-2})$
$q_{1\beta}$	$4.0380*10^{-2}$	$2.6034*10^{-2}$	$(-1.1153*10^{-2}, 9.1913*10^{-2})$
δ_β	$-6.4251*10^{-2}$	$4.3556*10^{-2}$	$(-1.5047*10^{-1}, 2.1965*10^{-2})$
c_1	$-2.1129*10^{-1}$	$3.4767*10^{-2}$	$(-2.8011*10^{-1}, -1.4247*10^{-1})$
b_1	$4.3934*10^{-3}$	$4.2247*10^{-2}$	$(-7.9232*10^{-2}, 8.8019*10^{-2})$
a_1	17.0000	$3.2273*10^{-5}$	(16.9999, 17.0001)
$p_{2\alpha}$	$7.5344*10^{-3}$	$6.2848*10^{-4}$	$(6.2904*10^{-3}, 8.7785*10^{-3})$
$q_{2\alpha}$	$-2.6222*10^{-1}$	$1.7885*10^{-1}$	$(-6.1625*10^{-1}, 9.1799*10^{-2})$
$p_{2\beta}$	$2.5499*10^{-3}$	$3.6616*10^{-4}$	$(1.8251*10^{-3}, 3.2747*10^{-3})$
$q_{2\beta}$	$2.9692*10^{-2}$	$1.1815*10^{-2}$	$(6.3043*10^{-3}, 5.3080*10^{-2})$
c_2	$3.2030*10^{-2}$	$2.4806*10^{-2}$	$(-1.7072*10^{-2}, 8.1133*10^{-2})$
b_2	$1.8170*10^{-1}$	$3.7237*10^{-2}$	$(1.0799*10^{-1}, 2.5541*10^{-1})$
a_2	33.8456	$1.4437*10^{-4}$	$(33.8454, 3.3846*10^{1})$
p_3	$-2.2485*10^{-3}$	$4.3131*10^{-4}$	$(-3.1022*10^{-3}, -1.3947*10^{-3})$
q_3	$-3.3581*10^{-2}$	$4.0324*10^{-2}$	$(-1.1340*10^{-1}, 4.6237*10^{-2})$
c_3	$4.3093*10^{-1}$	$1.3511*10^{-1}$	$(1.6349*10^{-1}, 6.9836*10^{-1})$
b_3	$-4.5252*10^{-2}$	$1.0586*10^{-1}$	$(-2.5480*10^{-1}, 1.6429*10^{-1})$
a_3	21.0000	$2.6346*10^{-3}$	$(20.9948, 2.1005*10^{1})$
$R^2 = 0.962844$			

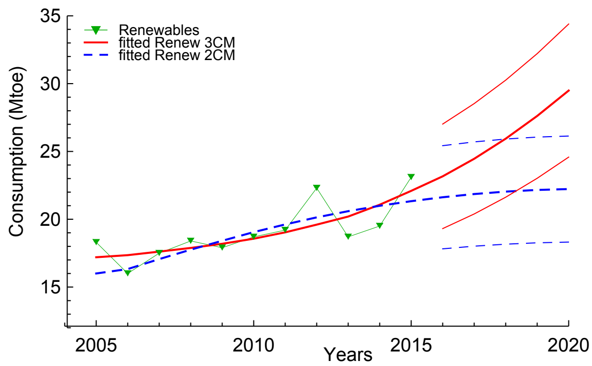

Figure 10: Sweden. Predictions and confidence bands for renewables for 3CM and 2CM.

Table 7: Sweden. Comparison between 2CM and 3CM: confidence band width, estimated standard deviation and p-value for the Kolmogorov–Smirnov test.

		2CM	3CM
${}_u\hat{\sigma}_2$		0.0874	0.0831
p-value		0.9440	0.9993
confidence band width	step 1	7.9424	7.7079
	step 2	8.2560	8.1385
	step 3	8.5769	8.6314
	step 4	8.8943	9.1891
	step 5	9.1950	9.8123

Table 8: Sweden. Comparison between 2CM and 3CM: forecasting accuracy measures.

Renewables	2CM					3CM				
	step 1	step 2	step 3	step 4	step 5	step 1	step 2	step 3	step 4	step 5
RMSE	7.024	9.087	7.485	6.616	7.458	6.071	7.497	7.595	5.046	1.923
MAPE	0.120	0.148	0.144	0.137	0.160	0.092	0.119	0.136	0.081	0.045
sMAPE	0.121	0.151	0.149	0.150	0.182	0.090	0.113	0.133	0.087	0.046
MASE	1.661	2.119	2.119	2.021	2.423	1.288	1.662	2.031	1.224	0.654
UMBRAE	1.503	1.604	3.450	1.309	1.908	1.069	1.249	3.531	0.614	0.602
% Better	29%	17%	0%	25%	0%	57%	50%	20%	50%	67%

Forecasting accuracy analysis results are given in Table 8. The results denote the superiority of the 3CM compared to the 2CM. Only at step 3 are RMSE and UMBRAE slightly larger for 3CM. All other measures show reduced values denoting a better forecasting performance for renewables with the 3CM.

4 Concluding remarks

The applications presented in this paper show the feasibility of the 3CM, which can be fitted to three connected time series, thus exploiting their relationship. Obviously, the 3CM is able to specifically describe both CGO and nuclear. Our results highlight that the third competitor, renewables, for which the same data are used for both models, takes advantage of the split between CGO and nuclear data. Similar encouraging results have been obtained also for other countries.

The 3CM proposed here could be further generalized by removing some constraints in the coefficient structure. In the model proposed here, we differentiated between internal WOM and external WOM for each competitor. However, external WOM from different competitors has been described with the same coefficient. Relaxing these assumptions and verifying whether this enrichment provides a significant improvement in data fitting will be the aim of our future research.

Acknowledgements

The work of the M.S.Zahangir has been supported by a grant of "Centro studi di Economia e Tecnica dell'Energia Giorgio Levi Cases," University of Padova.

References

Atkinson, K. E. (1962). *An Introduction to Numerical Analysis. 2nd ed.* Wiley, New York.

Bass, F. M., Krishnan, T. V., and Jain, D. C. (1994). "Why the Bass model fits without decision variables". *Marketing Science*, 13, 3, pp. 203–223.

Boswijk, H. P. and Franses, P. H. (2005). "On the econometrics of the Bass diffusion model". *Journal of Business & Economic Statistics*, 23, 3, pp. 255–268.

British Petroleum (2016). BP statistical review of world energy 2016. Available <www.bp.com> [accessed 21.10.16].

Chen, C., Twycross, J., and Garibaldi, J. M. (2017). "A new accuracy measure based on bounded relative error for time series forecasting". *PLoS ONE*, 12(3), pp. 1–23.

Dalla Valle, A. and Furlan, C. (2011). "Forecasting accuracy of wind power technology diffusion models across countries". *International Journal of Forecasting*, 27, 2, pp. 592–601.

Dalla Valle, A. and Furlan, C. (2014). "Diffusion of nuclear energy in some developing countries". *Technological Forecasting and Social Change*, 81, pp. 143–153.

Darda, M. A., Guseo, R., and Mortarino, C. (2015). "Nonlinear production path and an alternative reserves estimate for South Asian natural gas". *Renewable and Sustainable Energy Reviews*, 47, pp. 654–664.

Furlan, C., Guidolin, M., and Guseo, R. (2016). "Has the Fukushima accident influenced short-term consumption in the evolution of nuclear energy? An analysis of the world and seven leading countries". *Technological Forecasting and Social Change*, 107, pp. 37–49.

Furlan, C. and Mortarino, C. (2018). "Forecasting the impact of renewable energies in competition with non-renewable sources". *Renewable and Sustainable Energy Reviews*, 81(2), pp. 1879–1886.

Guidolin, M. and Guseo, R. (2012). "A nuclear power renaissance?". *Technological Forecasting and Social Change*, 79, 9, pp. 1746–1760.

Guidolin, M. and Guseo, R. (2016). "The German energy transition: Modeling competition and substitution between nuclear power and renewable energy technologies". *Renewable and Sustainable Energy Reviews*, 60, pp. 1498–1504.

Guidolin, M. and Mortarino, C. (2010). "Cross-country diffusion of photovoltaic systems: Modelling choices and forecasts for national adoption patterns". *Technological Forecasting and Social Change*, 77, 2, pp. 279–296.

Guseo, R. (2011). "Worldwide cheap and heavy oil productions: A long-term energy model". *Energy Policy*, 39, 9, pp. 5572–5577.

Guseo, R. and Dalla Valle, A. (2005). "Oil and gas depletion: diffusion models and forecasting under strategic intervention". *Statistical Methods and Applications*, 14, 3, pp. 375–387.

Guseo, R., Dalla Valle, A., and Guidolin, M. (2007). "World oil depletion models: Price effects compared with strategic or technological interventions". *Technological Forecasting and Social Change*, 74, 4, pp. 452–469.

Guseo, R. and Mortarino, C. (2014). "Within-brand and cross-brand word-of-mouth for sequential multi-innovation diffusions". *IMA Journal of Management Mathematics*, 25, 3, pp. 287–311.

Guseo, R. and Mortarino, C. (2015). "Modeling competition between two pharmaceutical drugs using innovation diffusion models". *The Annals of Applied Statistics*, 9, 4, pp. 2073–2089.

Guseo, R., Mortarino, M., and Darda, M. A. (2015). "Homogeneous and heterogeneous diffusion models: Algerian natural gas production". *Technological Forecasting and Social Change*, 90 (B), pp. 366–378.

Hyndman, R. J. and Koehler, A. B. (2006). "Another look at measures of forecast accuracy". *International Journal of Forecasting*, 22, pp. 679–688.

Marchetti, C. and Nakicenovic, N. (1979). *The dynamics of energy systems and the logistic substitution model*. International Institute for Applied Systems Analysis, Research Report RR-79-013, Laxenburg, Austria.

Peres, P., Muller, E., and Mahajan, V. (2010). "Innovation diffusion and new product growth models: A critical review and research directions". *International Journal of Research in Marketing*, 27, pp. 91–106.

Seber, G. and Wild, C. (2003). *Nonlinear Regression*. Wiley, New York.

Tashman, L. J. (2000). "Out-of-sample tests of forecasting accuracy: an analysis and review". *International Journal of Forecasting*, 16, pp. 437–450.

Working Paper Series
Department of Statistical Sciences, University of Padua

You may order paper copies of the working papers by emailing wp@stat.unipd.it
Most of the working papers can also be found at the following url: http://wp.stat.unipd.it

UNIVERSITA DEGLI STUDI DI PADOVA
DIPARTIMENTO DI SCIENZE STATISTICHE

Department of Statistical Sciences
University of Padua
Italy